General source and receiver positions in coarse-grid finite-difference schemes

Rune Mittet, Sting Research, and Børge Arntsen, Statoil

Summary

Coarse grid finite-difference schemes do not allow for general source and receiver positions. This problem is here solved using optimized operators with general phase-shift properties. These operators are band-limited representations of the Dirac delta function and the derivative of the Dirac delta function. The scheme is tested for a single source and a small source array. The resulting finite-difference solution is for both cases close to the analytical solution.

Introduction

Coarse-grid methods like pseudo-spectral methods (Fornberg, 1975); (Kosloff and Baysal, 1982) or high order finite-difference methods (Holberg, 1987) are ideally suited for implementing fast and memory efficient 3-D elastic modeling schemes (Mittet et al., 1988); (Reshef et al., 1988). These methods require few nodes per shortest wavelength in order to describe a propagating wave field, thus both storage requirements and the number of numerical calculations are reduced as compared to low order finite-difference schemes. However, there are problems implementing the source function when the typical distance between adjacent grid points is of order 10 m. Even a single air gun can not be correctly implemented, unless the true source depth coincide with a grid node. Assuming a grid spacing of 10 m, then the source must be placed at the depth of 10 m since there are no nodes between the free surface and this depth. If the true depth of the source is 4 m, then the ghost contribution cannot be properly described using a coarse grid. The problem is even larger if a marine source array is to be simulated. A conventional marine source array consists of a number (from 5 to 70) of individual air guns, typically separated by 1 - 4 m. This implies that effective point-source signatures estimated from measurements cannot be implemented directly in a coarse-grid finite-difference scheme. An approximate solution to this problem is to generate effective sources at chosen node positions (Landrø et al., 1993) which must be calculated by an inversion procedure prior to the finite-difference modeling.

Here we present a method which obviates this inversion based preprocessing of the source contribution and include the source contribution directly at the true depth, independently of the grid spacing. The new scheme also allows for arbitrary receiver positions. The method is based on generating optimized band-limited approximations to the Dirac delta function and its first derivative, where these band-limited functions are designed with a general phase shift. The resulting operators represent a generalization of the operators given by Holberg (1987).

The band-limited Dirac delta function is identical with the convolution phase-shift operator. This implies that if a regularly sampled function is known and within required wavenumber limits, then the response at any location can be calculated using the optimized phase-shift operator. Simulating a real experiment, group summation can be performed during modeling and in addition a streamer with variable depth and feathering may be simulated.

The acoustic and elastic Kirchhoff integrals require that proper approximations for the monopole and dipole source terms are known. Thus, good approximations to these operators can increase the accuracy of reverse time migration schemes when the recorded field is not sampled with a constant interval or the receiver depths do not coincide with the grid.

Theory

For simplicity we discuss the implementation of the optimized phase-shift source and receiver operators using the 3D acoustic wave equation, but the operators can be implemented directly in a 3D staggered-grid elastic finite-difference scheme. In the following, the Einstein summation convention is used. The acoustic wave equation for forward modeling with a source signature $S(t)$ is,

$$\partial_t^2 P(\boldsymbol{x},t|\boldsymbol{x}_s) - M(\boldsymbol{x})\partial_j\{\rho^{-1}(\boldsymbol{x})\partial_j P(\boldsymbol{x},t|\boldsymbol{x}_s)\} = \delta(\boldsymbol{x}-\boldsymbol{x}_s)S(t), \quad (1)$$

where $P(\boldsymbol{x},t|\boldsymbol{x}_s)$ is the pressure due to a source at $\boldsymbol{x}_s$, $\rho(\boldsymbol{x})$ is the density and $M(\boldsymbol{x})$ is the bulk modulus.

The monopole operator needed in the source term of the wave equation is an approximation to the Dirac delta function,

$$\delta(x-x_s). \quad (2)$$

The Dirac delta function is identical with the convolution phase-shift operator $s_x^{\delta x}$,

$$\begin{aligned}\phi(x+\delta x) &= \int_{-\infty}^{\infty} dx'\{\delta(x'-\delta x)\}\phi(x+x') \\ &= s_x^{\delta x} * \phi(x). \quad (3)\end{aligned}$$

A proper discrete version of the convolution phase-shift operator makes it possible to simulate sources and receivers at arbitrary grid positions.

Assume that the operator can be band limited and is to be used on a regularly sampled function with sampling

interval Δx. Let $x = i\Delta x$ with i integer. Let $\delta x = \eta\Delta x$ with η a real number such that $-0.5 \leq \eta \leq 0.5$. The discrete version of $s_x^{\delta x}$ is denoted S_x^η,

$$\begin{aligned}\phi(j\Delta x + \eta\Delta x) &= S_x^\eta \phi(j\Delta x) \\ &= \sum_{l=-L}^{L} [\Delta x \delta(l\Delta x - \eta\Delta x)]\phi(j\Delta x + l\Delta x) \\ &= \sum_{l=-L}^{L} \beta_l^\eta \phi_{j+l}. \end{aligned} \quad (4)$$

The Fourier response of S_x^η is,

$$S^\eta(k) = \sum_{l=-L}^{L} \beta_l^\eta e^{ik(l-\eta)\Delta x}. \quad (5)$$

Let the response of $S^\eta(k)$ be represented by,

$$S^\eta(k) = 1 + \varepsilon^\eta(k) \quad (6)$$

where $\varepsilon^\eta(k)$ is the relative error in frequency response of the operator S_x^η. The derivative of the frequency response of $S^\eta(k)$ is,

$$\partial_k S^\eta(k) = \partial_k \varepsilon^\eta(k). \quad (7)$$

The group velocity criterion (Holberg, 1987) can be used for the phase-shift operator. If it is required that $S^\eta(k)$ is as close as possible to 1 and close to equiripple, that is, the derivative of $S^\eta(k)$ with respect to k is as close to 0 as possible, then,

$$\begin{aligned}&\min(S^\eta(k) - 1 + k\partial_k S^\eta(k)) = \\ &\min(\varepsilon^\eta(k) + k\partial_k \varepsilon^\eta(k)) = \\ &\min(\varepsilon^\eta_{gr}(k)). \end{aligned} \quad (8)$$

The error functional $\mathcal{E}_L^\eta$ used her is,

$$\begin{aligned}\mathcal{E}_L^\eta &= [\int_{k=0}^{K_m} dk (S^\eta(k) - 1 + k\partial_k S^\eta(k))^2 \\ &+ w(\sum_{l=-L}^{L} \beta_l^\eta - 1)]^2 \end{aligned} \quad (9)$$

where

$$\begin{aligned}&S^\eta(k) - 1 + k\partial_k S^\eta(k) = \\ &\sum_{l=-L}^{L} \{\beta_l^\eta [1 + ik(l-\eta)\Delta x] e^{ik(l-\eta)\Delta x}\} \quad - 1. \end{aligned} \quad (10)$$

The term proportional to w in equation (9) ensures that the sum of all phase-shift operator coefficients is equal to 1. This constraint must be implemented to give operators with a proper amplitude preserving behavior for the dc components. The dipole (derivative) operator is generated by the same procedure as described here for the monopole (phase-shift) operator.

With these operators, a staggered-grid high-order modeling scheme can be implemented. Let $x = i\Delta x$, $y = j\Delta y$, $z = k\Delta z$ and $t = n\Delta t$,

$$\begin{aligned}A_{i+\frac{1}{2},j,k} &= \rho^{-1}_{i+\frac{1}{2},j,k} \partial_x^+ P^n_{i,j,k}, \\ B_{i,j+\frac{1}{2},k} &= \rho^{-1}_{i,j+\frac{1}{2},k} \partial_y^+ P^n_{i,j,k}, \\ C_{i,j,k+\frac{1}{2}} &= \rho^{-1}_{i,j,k+\frac{1}{2}} \partial_z^+ P^n_{i,j,k}, \end{aligned} \quad (11)$$

and,

$$\begin{aligned}U_{i,j,k} &= M_{i,j,k} \partial_x^- A_{i+\frac{1}{2},j,k}, \\ V_{i,j,k} &= M_{i,j,k} \partial_y^- B_{i,j+\frac{1}{2},k}, \\ W_{i,j,k} &= M_{i,j,k} \partial_z^- C_{i,j,k+\frac{1}{2}}, \end{aligned} \quad (12)$$

where ∂_i^+ and ∂_i^- are high-order forward and backward derivative operators in the i-direction respectively (Holberg, 1987). A second order time integration of the scheme gives,

$$\begin{aligned}P^{n+1}_{i,j,k} &= 2P^n_{i,j,k} + P^{n-1}_{i,j,k} + U_{i,j,k} + V_{i,j,k} + W_{i,j,k} \\ &+ \mathcal{D}_{I,J,K} S^n, \end{aligned} \quad (13)$$

where $\mathcal{D}$ is the spatial part of the source term. This term is a band-limited approximation to the 3D Dirac delta function,

$$\delta(\boldsymbol{x} - \boldsymbol{x}_s) = \delta(x - x_s)\delta(y - y_s)\delta(z - z_s), \quad (14)$$

and can be constructed from the coefficients β_l^η. The capital index $I(i, i_s, \eta_s)$ depends on i, i_s, η_s so that,

$$\begin{aligned}x &= i\Delta x, \\ x_s &= (i_s + \eta)\Delta x, \end{aligned} \quad (15)$$

and likewise for the capital indices J and K.

This implies that S^n, the contribution from the temporal source term at time $n\Delta t$, in principle is distributed over several nodes in all spatial directions and such that this three dimensional band-limited delta-function approximation is centered at the true source position $\boldsymbol{x}_s$ and not at the nearest node. The coefficients of $\mathcal{D}_{I,J,K}$ are scaled with the steplengths such that if $\boldsymbol{x}_s$ coincides with a node position then,

$$\mathcal{D}_{I,J,K} = \frac{1}{\Delta x}\frac{1}{\Delta y}\frac{1}{\Delta z}. \quad (16)$$

at this node and zero for the neighboring nodes.

For recording purposes a direct 3D generalization of equation (4) can be used,

$$\begin{aligned}&P^n(x_r, y_r, z_r) = \\ &S_x^{\eta_x} S_y^{\eta_y} S_z^{\eta_z} P_{i,j,k} = \\ &\sum_{l_x=-L_x}^{L_x} \sum_{l_y=-L_y}^{L_y} \sum_{l_z=-L_z}^{L_z} \beta_{l_x}^{\eta_x} \beta_{l_y}^{\eta_y} \beta_{l_z}^{\eta_z} P_{i+l_x, j+l_y, k+l_z}. \end{aligned} \quad (17)$$

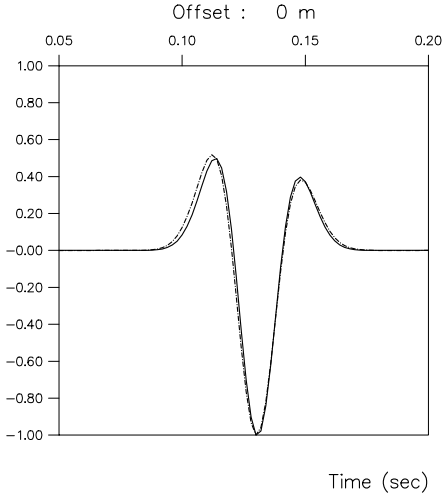

Fig. 1: Pressure at depth 100m. Zero offset. Solid line : analytical solution for source at 4 m. Dashed-dotted line : finite-difference solution for source at 10 m.

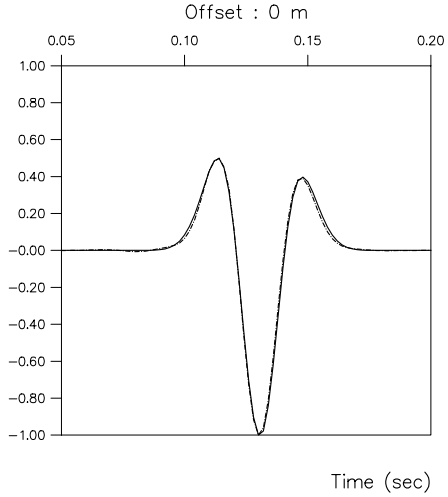

Fig. 2: Pressure at depth 100m. Zero offset. Solid line : analytical solution for source at 4 m. Dashed-dotted line : finite-difference solution for source at 4 m.

The operator half lengths L_{x_i} are usually of order 8-10 to ensure high numerical precision for all phase shifts. The computer time needed to perform this triple sum is normally small compared to the the computer time needed to step the wavefield forward in time since the number of receivers usually is much less than the total number of grid nodes and recording is not necessary at each time step in order to sample the field properly.

The operators for both sources and receivers take the form of 2D tables. Each source or receiver position has nearest node coordinates for each spatial dimension and η coordinates giving the distance from the nearest node to the true source or receiver coordinate. The operator table contain a set of operators with length $2L + 1$ for each η-value. The η steplengths can be made arbitrarily fine since the table has to be built only once.

Numerical example

The proposed band-limited delta-function operators are put to two tests. The first test is for a single source located at a true depth of 4 m. The recording is performed at a depth of 100 m. The finite-difference node spacing is 10 m. The P-wave velocity is 1480 m/s and the density is 1.0 g/cm^3. In Figure 1 the analytical solution is plotted with a solid line. The dashed-dotted line is the result of a finite-difference simulation where the source is assumed to be located at the nearest node. The optimized spatial delta functions is not used in this simulation. Thus, in the finite-difference simulation the source depth becomes 10 m. As can be seen, the two signals deviate. Part of this deviation is due to the travel-time difference of the direct signal and some of the difference is due to a different ghost effect for the finite-difference solution compared to the true solution.

In Figure 2 the analytical solution is plotted with a solid line. The dashed-dotted line is the result of a finite-difference simulation where the source is placed at the true depth using the optimized spatial delta functions. The fit is clearly improved compared to the simple source implementation approach discussed for Figure 1. We find this improved fit for all offsets.

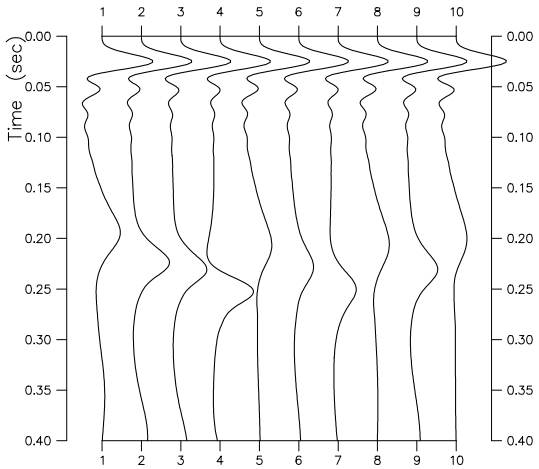

Fig. 3: Notional source signatures for the 10 air guns in the source array.

The second test is a comparison of the finite-difference solution and the analytical solution for a small source array where the effective source signatures (notional source signatures) are known. The 10 air-gun signatures are shown in Figure 3. The frequency content of the original signatures was reduced to 50 Hz, without changing the waveforms. In Figure 4 the analytical solution is plotted with a solid line. The dashed-dotted line is the result of a finite-difference simulation where the optimized spatial delta functions are not used. This implies that all sources are located at the nearest node in the finite-difference simulation. Deviations can be seen in the arrival time and

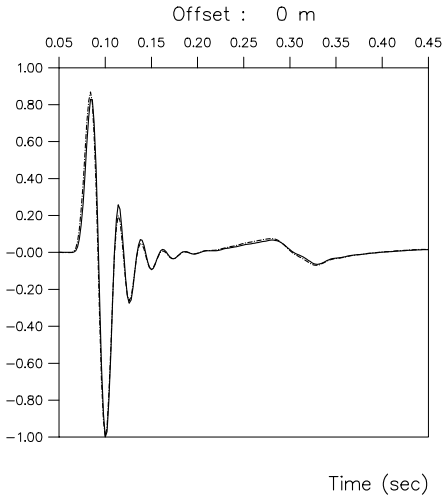

Fig. 4: Pressure at depth 100m. Zero offset. Solid line : analytical solution for source array. Dashed-dotted line : finite-difference solution for individual sources at nearest node in finite-difference grid.

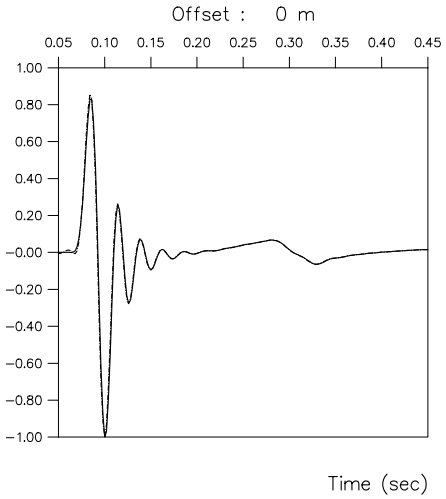

Fig. 5: Pressure at depth 100m. Zero offset. Solid line : analytical solution for source array. Dashed-dotted line : finite-difference solution for individual sources at true positions.

amplitude of the primary part of the signal and also for the part related to the first bubble oscillation. The errors are comparable to those in Figure 1, but a different time scale is used in Figure 4 to include the first bubble oscillation

In Figure 5 the analytical solution (solid line) together with the result of a finite-difference simulation where the sources are placed at their true x-, y- and z-coordinates using the optimized spatial delta functions (dashed-dotted line) are shown. The fit is clearly improved compared to the strategy of using the nearest nodes as the source positions.

Conclusions

A method for positioning sources and receivers at arbitrary locations for coarse-grid finite-difference schemes have been presented. The method is based on designing optimized band-limited approximations for both the Dirac delta function and the spatial derivative of the Dirac delta function. These operators can have a general phase shift which allows the operator to be centered anywhere between grid nodes. The phase-shift operator used for recording at an arbitrary position is identical to the spatially band-limited delta function (monopole) used in the source term. The phase-shift derivative operator is identical to the spatially band-limited derivative of the delta function (e.g., dipole term in the Kirchhoff integral).

The optimized phase-shift operators were tested both for a single source and a small source array. Good agreement between the finite-difference solution and the analytical solution where found for all offsets in both cases.

Acknowledgments

This work has been financially supported by Statoil Research. We thank Statoil Research for the permission to publish this paper. We also wish to thank Martin Landrø who has supplied the notional source signatures for the source array.

References

Fornberg,B., 1975, On a Fourier method for the integration of hyperbolic equations: Soc.Ind.Appl.Math., J.Numer.Anal., 509–528.

Holberg, O., 1987, Computational aspects of the choice of operator and sampling interval for numerical differentiation in large-scale simulation of wave phenomena: Geophys. Prosp., **37**, 629–655.

Kosloff, D., and Baysal, E., 1982, Forward modeling by a Fourier method: Geophysics, **47**, 1402–1412.

Landrø M., Mittet, R., and Sollie, R., 1993, Implementing measured source signatures in a coarse-grid finite-difference modeling scheme: Geophysics, **58**, 1852–1860.

Mittet, R., Holberg, O., Arntsen, B., and Amundsen, L., 1988, Fast finite-difference modeling of 3-D elastic wave propagation: 58th Ann. Internat. Mtg., Soc. Expl. Geophys., 1308–1311.

Reshef, M., Kosloff, D., Edwards, M., and Hsiung, C., 1988, Three dimensional acoustic modelling by the Fourier method: Geophysics, **53**, 1175–1183.